Myocardial Mechanics in Aortic and Mitral Valvular Regurgitation: the Concept of Instantaneous Impedance as a Determinant of the Performance of the Intact Heart

CHARLES W. URSCHEL, JAMES W. COVELL, EDMUND H. SONNENBLICK, JOHN ROSS, JR., and EUGENE BRAUNWALD

From the Cardiology Branch, National Heart Institute, Bethesda, Maryland 20014

ABSTRACT The effects on myocardial mechanics of acute, artificial aortic and mitral regurgitation were studied in the dog to determine the manner in which the changes in load induced by valvular regurgitation alter ventricular performance. With mitral and aortic regurgitant volumes of approximately the same magnitude as the forward stroke volume, immediate increases occurred in total stroke volume, left ventricular end-diastolic pressure, and peak ejection velocity, whereas contractility remained unchanged. Although calculated myocardial fiber tension rose, the rate of decline of tension during ejection was accelerated with regurgitation due to the more rapid decrease in ventricular size. Average tension therefore decreased relative to average pressure. As a consequence of the increased fiber length and this unloading, contractile element velocity, work, and power were increased. Despite unchanged contractility of the myocardium, the ejection fraction rose with both aortic and mitral regurgitation.

When regurgitant beats were compared with control beats at a constant end-diastolic volume, ventricular stroke volume, work, power, and ejection fraction, as well as contractile element velocity, work, and power consistently increased. Thus, reduction of instantaneous impedance to ejection allowed the ventricle to empty further, reducing ventricular wall tension with a resultant increase in the velocity of shortening. External energy output was increased despite unchanged contractility and diastolic fiber length. It is concluded that the impedance to ejection and myocardial fiber tension during ejection govern the velocity and extent of contractile element shortening, and hence affect stroke volume, peak aortic flow rate, and ejection fraction. The alterations of ventricular function accompanying valvular regurgitation can be explained by an evaluation of the effects of these lesions on the instantaneous impedance to left ventricular ejection.

Received for publication 5 June 1967 and in revised form 14 November 1967.

INTRODUCTION

During the past decade there has been considerable interest in defining the hemodynamic consequences of aortic and mitral valvular regurgitation. The most commonly employed approach, both in experimental and clinical studies, has been to determine the effects of these lesions on intracardiac pressures, ventricular volumes, and cardiac output. In some studies, attempts have also been made. to measure the volume of regurgitant flow (1–3) and the effects of known quantities of valvular regurgitation on cardiovascular dynamics have been determined (4–6). Angiocardiographic methods have been utilized to determine the ventricular end-diastolic volume and the ejection fraction in patients with valvular regurgitation (7–9). In experimental studies on the effects of acutely induced, metered regurgitant flow (4, 5), it was

shown that mitral regurgitation produced only a slight lowering of the effective left ventricular function curve, whereas equivalent degrees of aortic regurgitation produced more striking depression. Although all of these studies have provided considerable information concerning the pumping functions of the left ventricle, they have yielded only limited insight into the mechanisms and consequences of the mechanical burdens induced by valvular regurgitation on the myocardium. Moreover, they have not distinguished completely the effects of the altered load placed on the myocardium (10–13) by the valvular lesion from possible depression in the intrinsic contractile state of the myocardium.

The recent application of the principles of muscle mechanics, as developed in isolated heart muscle preparations, to the study of the contractile state of the intact ventricle (14–16) offers a more direct means for the evaluation of myocardial performance in the presence of abnormal hemodynamic loads. This approach requires simultaneous consideration of those major factors which alter myocardial performance: (*a*) the preload, as reflected by the ventricular end-diastolic volume, (*b*) the afterload, as reflected by the ventricular systolic tension, and (*c*) the inotropic state of the myocardium, as reflected by the position of the force-velocity curve. In the present investigation, these concepts were applied in an examination of the effects of acutely induced, metered aortic–left ventricular flow to simulate aortic regurgitation and left ventricular–left atrial regurgitation to simulate mitral regurgitation.

METHODS

17 dogs, ranging in weight from 15.5 to 25.6 kg (average, 20.4 kg) were anesthetized with i.v. sodium pentobarbital, 30–40 mg/kg, and a bilateral thoracotomy was performed under positive pressure respiration. The experimental preparation is illustrated in Fig. 1. The probe [1] of an electromagnetic flowmeter was placed about the aortic root. A stainless steel, right angle cannula (0.8 cm I.D.) was placed into the left ventricular cavity through a stab wound in the apical dimple. An external flow probe [2] was placed into this circuit, and a glass T tube distal to the flow probe allowed diversion of blood flow through one of two paths. The first, circuit *A* in Figure 1, led to the left atrium; blood flowing from the left ventricle through this pathway will be referred to as "mitral insufficiency flow" (MI). The second limb of the T tube connected the left ventricle with the aorta through a cannula in the left subclavian artery (circuit *B* in Fig. 1). A ball-valve in this circuit permitted flow to occur only from the aorta to the left ventricle, and blood flowing through this pathway will be referred to as "aortic insufficiency flow" (AI).

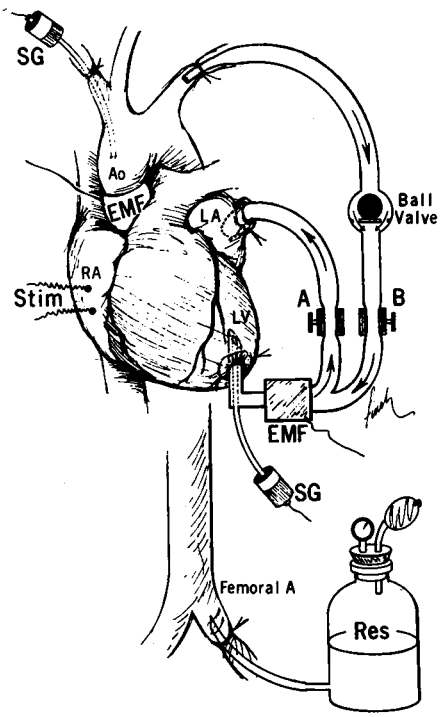

FIGURE 1 Experimental preparation: A stainless steel cannula was placed in the apex of the ventricle. By opening clamp *A*, blood was shunted from the left ventricle (*LV*) into the left atrium (*LA*) during systole, and by opening clamp *B* from the aorta (*Ao*) to the LV during diastole. The ball valve prevented flow from the LV to the Ao during systole. Aortic and shunt flows were metered with electromagnetic flow probes (*EMF*). Blood volume was controlled with a pressurized reservoir bottle (*Res*). Heart rate was controlled by an electrical stimulator (*Stim*). SG, pressure transducer.

Both aortic and shunt flows were measured with a two-channel gated sine wave flowmeter.[3] All flow measurements were corrected for the 10 msec time delay present in this instrument. Left ventricular (LV) pressure was measured with a Statham P23Db gauge, attached to a 1.5 mm I.D. steel cannula introduced into the LV cavity through the large apical cannula. LV pres-

[1] Statham model Q, Statham Laboratories, Inc., Los Angeles, Calif.

[2] Statham model QH, Statham Laboratories, Inc., Los Angeles, Calif.

[3] Statham model M 4000, Statham Laboratories, Inc., Los Angeles, Calif.

sure was recorded at two levels of amplification. At the higher sensitivity, left ventricular end-diastolic pressure could be determined to within ± 0.1 mm Hg. Aortic pressure was measured with a Statham P23Db gauge attached to a short length of No. 240 polyethylene tubing inserted into the arch of the aorta through the right subclavian artery. The first derivative of LV pressure, dp/dt, was determined with an R-C differentiating circuit exhibiting a constant phase shift of 90° ± 1° from 0 to 160 cps.

Blood volume, and, therefore, left ventricular end-diastolic pressure (LVEDP) and volume (LVEDV) were controlled by means of a pressurized reservoir connected to the cannulated left femoral artery. The experimental dog was cross-transfused with all donor blood before the experiment. After the sino-atrial node had been crushed, heart rate was maintained constant by stimulating the right atrium at a frequency of 125–140/min. A temperature probe was placed into the right atrium and temperature was maintained at 37°C by means of heating pads.

The effects of both AI and MI on LV function were studied in two ways. The first state consisted of rapidly opening the appropriate shunt after obtaining measurements during a stable control period, without regulating LVEDP or LVEDV. This was termed "free" AI or MI. Since opening the shunt led to an elevation of these variables, the effects of AI or MI were also compared to control beats by transfusing the dog from the reservoir to obtain an equivalent LVEDV during a second control period, as had been present during AI or MI. This was termed AI or MI at identical preload.

In order to assure that comparisons between AI or MI and the control periods were not affected by alterations in myocardial contractility, three techniques were used to test for and prevent changes in contractility. First, the force-velocity relation was calculated either during the isovolumic portion of an ejecting beat, or during completely isovolumic beats produced by sudden diastolic occlusion of the aorta, as previously described (17). By extrapolating the force-velocity relation to zero tension, maximum velocity of shortening (V_{max}) was obtained. V_{max} calculated in this manner has been shown to be a sensitive index of contractility (17, 18). Second, wall tension was calculated and plotted as a function of left ventricular mid-wall circumference. It has been shown in isolated papillary muscle (19), as well as in the intact heart (20, 21), that for a given state of contractility, isotonic or auxotonic contractions will shorten to and along the isovolumic length-tension curve. Finally, to obviate reflex changes in contractility, five dogs, three in which the effects of AI and MI were examined, and two with AI alone, were studied before and after beta-adrenergic blockage was induced with i.v. propranolol (5 mg).[4]

[4] Propranolol was supplied through the courtesy of Dr. A. Sahagian-Edwards of Ayerst Laboratories, New York.

Calculations and assumptions

Left ventricular pressure (LVP), the derivative of LVP (dp/dt), aortic flow, and shunt flow were measured at 10 msec intervals during representative ejecting beats. LVEDV was determined from the LVEDP and the pressure-volume curve of the potassium-arrested heart, obtained upon completion of the experiment, as previously described (16). The validity of this method is based on the assumption that ventricular diastolic compliance is unchanged by the intervention employed. In order to assure that this is the case, the length of a segment of the left ventricle was measured with a continuously recording caliper gauge (14) in seven dogs, and it was observed that neither AI or MI altered the relation between LVEDP and segment length. In addition, studies examining the relationship between LVEDV determined by the passive–pressure-volume curve and by biplane cineangiography are currently under way. Preliminary results of these studies have shown that there is an excellent correlation between the two techniques. In 24 observations obtained over a wide range of filling pressures and volumes (20–100 ml), LVEDV when determined by the pressure-volume curve technique correlated closely ($r = 0.821$) and averaged 1.6 ± 5 (SD) ml less than those obtained by cineangiography.

Instantaneous ventricular volume at a given instant during ejection was calculated as the difference between LVEDV and the accumulated flow to that instant. The LV was considered to be a thick-walled sphere. Assuming an even distribution of LV muscle, external volume was taken as the sum of LVEDV and muscle volume, and the radii of the external and internal volumes were computed, with the ventricular wall thickness comprising their difference. LV muscle volume was estimated from the postmortem weight of the LV including the septum. Although the degree to which the septum functionally behaves as LV wall is not definitely defined, wherein comparisons are made between interventions in the same heart as in the present study, the uncertainty thereby introduced is in the magnitude rather than in the direction of calculated changes. Assuming that stress is equal at all radii across the ventricular wall, i.e. a square wave stress distribution, it can be shown that this average stress or tension ($T = g/cm^2$) is equal to $PR_i/2h$, where R_i = internal

radius, and h = ventricular wall thickness, both in centimeters. In brief, this derivation assumes that the total force to be supported by the ventricular wall is equal to the product of the LVP and the internal surface area of the ventricle and derives the necessary supporting force in the wall (14, 22, 23).

The errors inherent in the use of a thick-walled sphere to approximate the normal left ventricle must be assessed in relative terms, since precise equations for wall tension cannot yet be derived even for more exact geometrical approximations of the ventricle. Two major sources of error are inherent in the use of the thick-walled sphere as a model. First, the equation for wall tension is derived for a thin-walled sphere. When derived correcting for wall thickness circumferential tension (g/cm^2) is described by the equation $PR_i^2/(R_o^2 - R_i^2)$ where R_o is the external radius. Wall tensions were calculated using $PR_i/2h$ because of the increased computational difficulties necessary to differentiate the second equation. $PR_i/2h$ overestimates wall tension by the factor $1 + h/R_i$. The magnitude of the overestimation will therefore depend on ventricular size and will be greatest at small ventricular volumes. The accelerated decline in wall tension calculated in this study due to more complete ventricular emptying (vide infra) would therefore be even more pronounced if the more precise expression had been employed.

Further, the equation $PR_i^2/R_o^2 - R_i^2$ provides only an approximation to "true" myocardial fiber tension, since factors such as the mode of coupling of pressure to the ventricular wall, the distribution of pressure and tension across the wall, and the role of tissue viscosity, and intramyocardial shear forces are not precisely defined.

A second potential source of inaccuracy from use of the sphere depends on the degree to which an ellipsoidal ventricle changes shape during ejection. If the length/diameter ratio remains constant, then circumferential tension would be overestimated to a constant degree using the spherical approximation. If the length/diameter ratio increased, as is known to occur with more complete ejection (24, 26), the overestimate due to the spherical approximation would be magnified.

The net result of the use of the thick-walled sphere model to calculate tension as $PR_i/2h$ is to underestimate the decrease in wall tension secondary to an increased ejection fraction. This provides a small error, however, over physiologic length/diameter ratios (27).

The equation used for calculating the mean velocity of circumferential fiber shortening of a thick-walled sphere was modified from that presented by Fry, Griggs, Jr., and Greenfield (14). For this derivation the ventricular wall is assumed to be composed of a series of concentric thin-walled spheres. The instantaneous velocity of circumferential shortening (V_{CF}) at the mid-wall can be calculated as

$$V_{CF}\ (cm/sec) = \frac{Q\ (cm^3/sec)}{2R_o \cdot R_i\ (cm^2)},$$

where Q = instantaneous flow rate out of the ventricle.

Circumferential velocities will be underestimated using the sphere as compared to an ellipsoid, increasingly so with a higher ejection fraction. Therefore where the effect of the intervention is to increase ejection fraction, calculations utilizing a sphere tend to underestimate slightly the magnitude of the actual changes which occur.

V_{CF} and T thus describe the velocity of shortening, and the force necessary to approximate the ends of a hypothetical 1.0 cm^2 cross-sectional area band of muscle encircling the ventricle at its mid-wall radius. All subsequent calculations describe the behavior of this hypothetical band.

Contractile element velocity (V_{CE}) was calculated by the model proposed by A. V. Hill (28) of a contractile element in series with an undamped spring (SE, series elastic). This model was proposed to explain the characteristic sudden shortening after an abrupt decrease in tension in a muscle fiber. Recent studies of the intact heart in which an identical quick release of tension can be achieved confirmed the applicability of the model (29). V_{CE} is the sum of V_{CF} and the velocity of elongation of the series elastic (V_{SE}). $V_{SE} = \frac{dT/dt}{kT}$, where kT equals the modulus of elasticity of the series elastic component of the muscle (30). The normalized value for k used in this study was 28, a value which is based upon observations on isolated heart muscle (30) and the intact heart (29). The calculated modulus of elasticity is independent of inotropic interventions or fiber length.

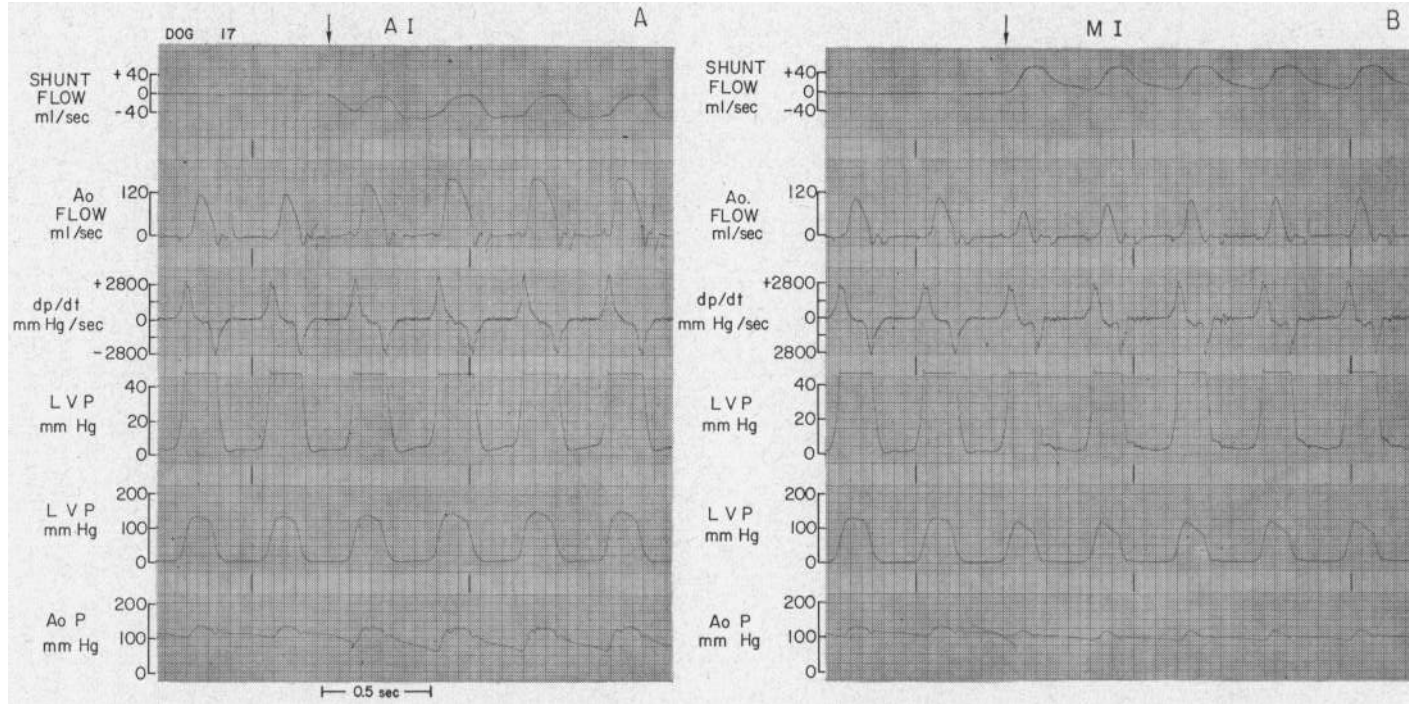

FIGURE 2 Tracings from a typical experiment: Recordings of shunt (regurgitant) flow, aortic flow (Ao Flow), first derivative of LV pressure (dp/dt), LV pressure (LVP) at high gain and low gain and aortic pressures (Ao P) are shown. At the arrows the aortic-LV shunt was opened (AI, panel A) and the left ventriculo-atrial shunt was opened (MI, panel B).

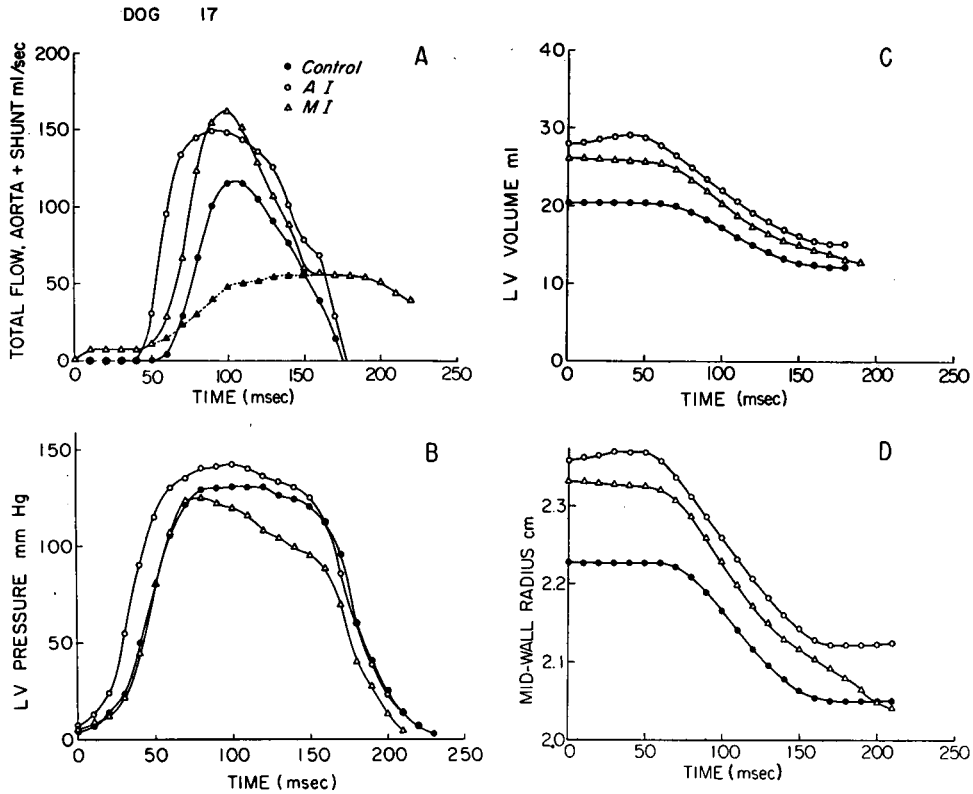

FIGURE 3 Myocardial mechanics comparing a control beat, free AI and free MI beats. In panel A the flow from LV to LA (MI flow) is shown by the closed triangles joined by the broken line.

Differentiation of the equation where $T = PR_i/2h$ and calculation of the velocity at the mid-wall yields:

$$V_{SE} = (R_i + h/2) \times \left[0.224(dp/dt)/P - \frac{Q}{56R_i^3} - \frac{Q}{56R_i^2} - \frac{Q}{56R_o^2}\right]$$

RESULTS

A. *Effects of free AI and MI.* Tracings from a typical experiment in which AI was produced (by opening circuit B in Fig. 1) are shown in Fig. 2A, and the data calculated from this experiment are shown in Figs. 3 and 4. Average values are presented in Table I. The total AI flow averaged 11.0 ml/stroke or 1.56 liter/min. This resulted in an elevation of the total stroke volume from an average of 12.1 to 19.9 ml, a smaller reduction of effective stroke volume from 12.1 to 8.9 ml, and an elevation of peak aortic flow (Fig. 3A). There was also an increase in the duration of ejection from 0.16 to 0.19 sec. AI did not alter left ventricular or aortic systolic pressures significantly, but as anticipated, reduced aortic diastolic and mean pressures (Table I). LVEDP (Fig. 3B), LVEDV (Fig. 3C) and LV mid-wall radius (Fig. 3D) rose consistently, and the ejection fraction increased, from an average of 0.43 to 0.55. The increase in aortic flow rate was accompanied by a relatively smaller rise in V_{CF} (Fig. 4A and Table I). The increase in LVEDV, occurring at a relatively constant LV systolic pressure, resulted in a significant rise in calculated wall tension (Fig. 4B), peak tension rising from 115 to 137 g/cm² and integrated tension (the area under the systolic tension-time curve) from 19.5 to 23.8 g sec/cm². V_{CE} before the opening of the aortic valve showed little change, but there was a substantial increase in V_{CE} during ejection (Fig. 4C and Table I). Since both V_{CE} and LV wall tension rose with AI, the product of these two variables, i.e. contractile element power, rose markedly, from an average peak value of 1149 to 1729 g cm/sec. The integral

of contractile element power, i.e. contractile element work, therefore also increased substantially, from 115 to 221 g cm.

Tracings from a typical experiment in which MI was produced by opening circuit A in Fig. 1 widely are shown in Fig. 2B, and the calculated data are shown in Figs. 3 and 4. The total MI flow produced was similar to the total AI flow and averaged 1.42 l/min, or 10.0 ml/stroke. The increases in total stroke volume, and total peak blood flow from the LV (the sum of forward plus regurgitant flow), ejection fraction, circumferential fiber velocity, and the reductions in forward stroke volume were also comparable to those observed in AI. However, the increases in LVEDP, LVEDV, and LV mid-wall radius were significantly less (Table I and Figs. 3B, C, and D). Whereas MI produced no significant change in LV or aortic peak systolic pressure, LV pressure tended to decline more rapidly during ejection than in either the absence of regurgitation or in AI (Fig. 3B). In contrast to AI, MI did not result in an elevation of LV wall tension; peak tension showed no significant change whereas integrated tension declined from 19.5 to 17.7 g sec/cm^2. Although V_{CE} and contractile element power rose with MI (Table I), these increases tended to be less than with AI.

B. *Effects of AI and MI at equivalent LVEDV.* In nine dogs AI or MI was compared with a second control period which followed transfusion to insure a comparable LVEDV. By this technique it was possible to determine the effects of the regurgitant lesion on myocardial mechanics without the added complication of an altered preload and therefore initial muscle length.

The results of a typical experiment with AI are shown in Fig. 5 and average results are shown in Table II. When AI was induced, LV systolic pressure fell slightly or was unchanged (Fig. 5A). LV volume declined more rapidly and to a greater extent in AI than during the control period (Fig. 5C), and V_{CF} (Fig. 5D and Table II) and V_{CE} (Fig. 5F and Table II) during ejection were higher, whereas peak and integrated LV wall tension were lower (Fig. 5E), and declined more rapidly than in the control beats. Since wall tension is a function of both ventricular pressure and

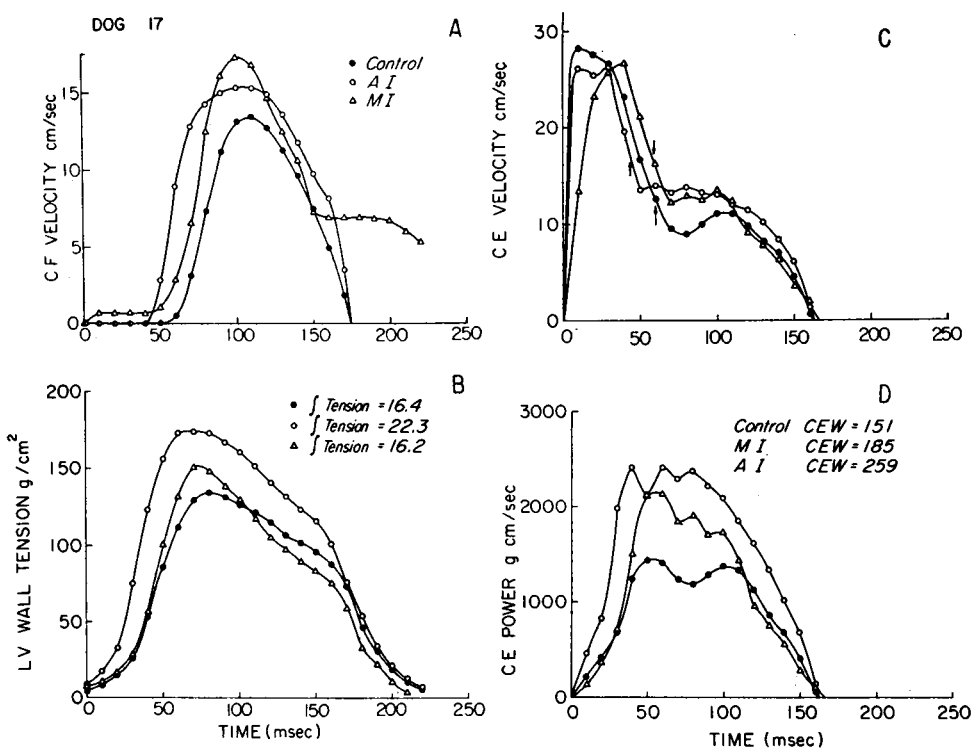

FIGURE 4 Comparison of a control beat, free AI and free MI.

TABLE I

Average Results from Six Experiments Comparing Free AI and MI

	Control	AI	MI
Aortic systolic pressure, *mm Hg*	110 ± 6	114 ± 5	108 ± 5
Aortic diastolic pressure, *mm Hg*	80 ± 8	60 ± 7*	76 ± 8*§
Aortic mean pressure, *mm Hg*	92 ± 7	84 ± 7‡	88 ± 7‡
LVEDP, *mm Hg*	4.3 ± 0.5	6.2 ± 0.7*	5.6 ± 0.7‡‖
LVEDV, *ml*	28.7 ± 3.0	36.4 ± 3.9*	32.7 ± 3.4‡δ
Heart rate	142 ± 4	142 ± 4	142 ± 4
Total stroke volume, *ml*	12.1 ± 1.6	19.9 ± 2.5*	19.8 ± 3.1*
Effective stroke volume, *ml*	12.1 ± 1.6	8.9 ± 0.7	9.8 ± 1.4*
Regurgitant stroke volume, *ml*	—	11.0 ± 2.6	10.0 ± 2.1
Effective cardiac index, *liter/min per m²*	2.14 ± 0.22	1.52 ± 0.09	1.72 ± 0.20
Regurgitant flow index, *liter/min per m²*	—	1.93 ± 0.42	1.76 ± 0.33
Ejection fraction, stroke volume/end-diastolic volume	0.43 ± 0.03	0.55 ± 0.02*	0.59 ± 0.04*
Total peak flow, *ml/sec*	116 ± 13	153 ± 16*	154 ± 17*
Aortic peak flow	116 ± 13	153 ± 16*	113 ± 12§
Duration of ejection, *sec*	0.16 ± 0.01	0.19 ± 0.01‡	0.14 ± 0.01*§
Mean systolic ejection rate *ml/sec*	76 ± 9	104 ± 12*	69 ± 8‡§
Peak LV wall tension, *g/cm²*	115 ± 9	137 ± 12*	119 ± 11§
Integrated LV wall tension, *g sec/cm²*	19.5 ± 1.9	23.8 ± 2.3*	17.7 ± 1.5‡§
Peak circumferential fiber-shortening velocity, *cm/sec*	10.78 ± 1.10	12.79 ± 1.02*	14.09 ± 1.53*
Peak contractile element velocity during ejection, *cm/sec*	10.01 ± 0.80	13.10 ± 0.86‡	12.55 ± 1.08*
Peak contractile element power, *g cm/sec*	1149 ± 148	1729 ± 210*	1519 ± 270‡
Contractile element work, *g cm*	151 ± 19	221 ± 26*	175 ± 27‡§
Circumferential fiber work, *g cm*	119 ± 16	190 ± 23*	173 ± 27*
Circumferential fiber work/contractile element work	0.79 ± 0.02	0.86 ± 0.01*	0.99 ± 0.01**§

Average levels (± SE) are shown for control, free AI, and free MI for six experiments.
The significance of changes is calculated by a paired t test, wherein the control to intervention differences from individual animals were averaged. t is then the average change divided by the SE of the average change (28).
* Comparing AI or MI with control, $P < 0.01$.
‡ Comparing AI or MI with control, $P < 0.05$.
§ Comparing AI with MI, $p < 0.01$.
‖ Comparing AI with MI, $P < 0.05$.

radius, and AI resulted in a more rapid decrease in ventricular volume during ejection (Fig. 5C), ventricular wall tension fell more rapidly than normal (Fig. 5E). These findings may be expressed as the ratio of integrated LV wall tension to integrated LV pressure, expressed in the same units (g/cm^2). This ratio averaged 1.36 during the control period and declined to 1.20 during AI. The ejection fraction rose from 0.40 to 0.65. Thus, when preload was held constant, AI resulted in a decrease in wall tension and concomitant increases in V_{CF}, V_{CE}, and the extent of fiber shortening.

Fig. 5B represents the relation between LV fiber length, expressed as mid-wall radius, and wall tension. The three solid squares represent the peak wall tensions observed at three initial lengths during isovolumic, i.e. nonejecting beats, whereas the three open squares represent similar data in the presence of AI. These six points all fell on the same length-active tension curve, suggesting that acute regurgitation did not alter the contractile state of the LV. Point "P" represents the relation between length and active tension in the same dog afer the administration of 10 mg of propranolol and illustrates how a reduction in contractility affects this relationship. Also shown in Fig. 5B are LV length-tension relations in two ejecting beats. Since aortic diastolic pressure is lower with AI, ejection begins at a lower wall tension than during the control beats, and with the more profound decline in length, wall tension declines further in AI than in the control period. In both the control and AI states, isovolumic contractions were used to describe a relation between peak ten-

sion and fiber length, and a curve could be drawn between these points. During ejection the fibers shortened to the same length-tension relation in all of the experiments, both during the control period and in the presence of AI. Subsequent shortening was usually along this same length-tension line, although the control beats tended to fall below the line more frequently in late ejection (Fig. 5B). Contractility was also evaluated by the extrapolation to zero tension of the force-velocity relation from isovolumic beats to obtain the maximum velocity of shortening of the unloaded contractile element (V_{max}) (17). Calculated V_{max} averaged 41 ± 2 cm/sec in the control period and was unchanged, 41 ± 2 cm/sec, with AI.

When MI was induced at a constant LVEDP (Table II), peak LV pressure declined (Fig. 6A). In contrast to AI, MI changed the contour of the tracing, the pressure reaching a peak in early systole and declining markedly during ejection (Fig.

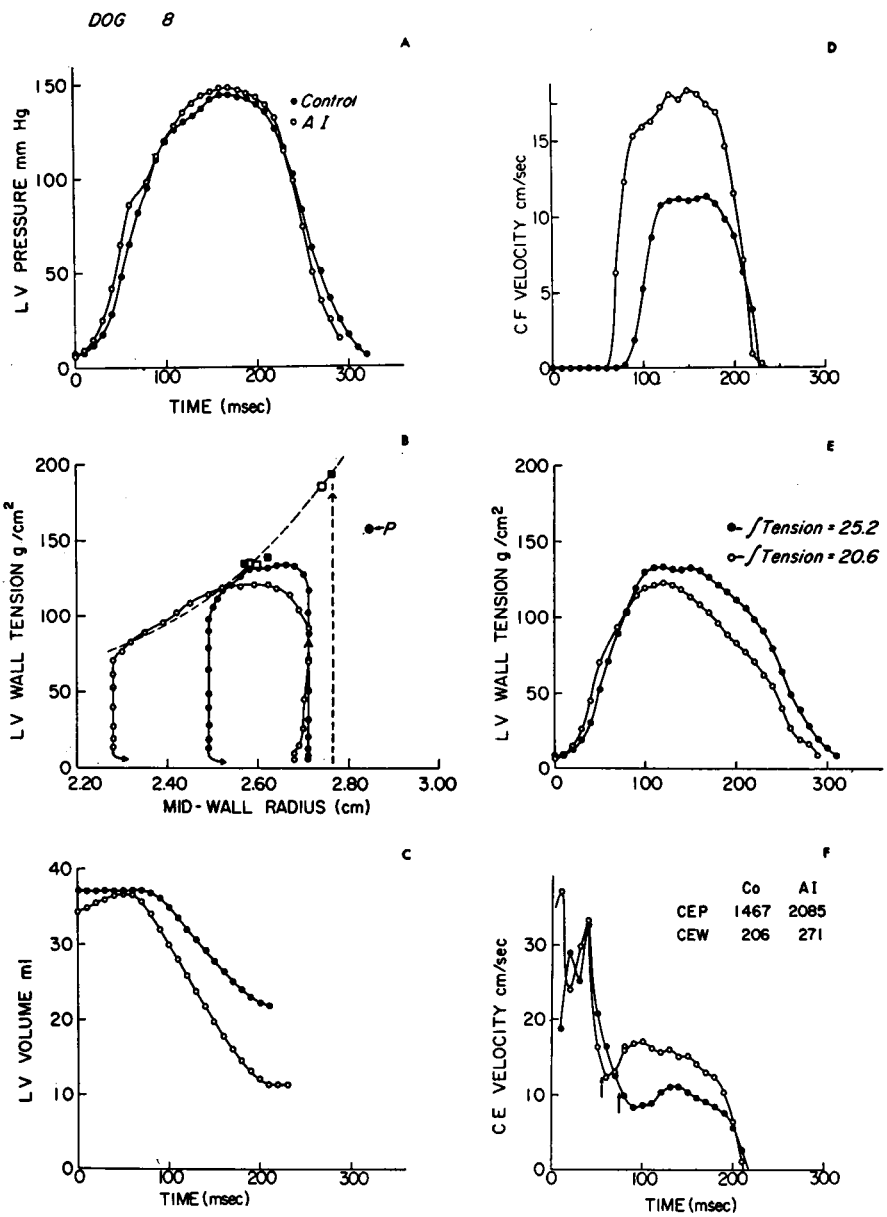

FIGURE 5 Comparison of a control beat and AI at the same end-diastolic volume.

TABLE II

Average Results Comparing the Effects of AI and MI at Equivalent Preloads

	Control	AI	Control	MI
Aortic systolic pressure, *mm Hg*	146 ± 8	134 ± 6*	121 ± 4	102 ± 5‡
Aortic diastolic pressure, *mm Hg*	104 ± 7	57 ± 5‡	87 ± 3	73 ± 5‡
Aortic mean pressure, *mm Hg*	121 ± 7	92 ± 5‡	101 ± 3	82 ± 5‡
LVEDV, *ml*	35.7 ± 3.6	35.4 ± 3.6	33.1 ± 2.7	33.1 ± 2.7
Total stroke volume, *ml*	13.1 ± 1.1	21.5 ± 1.2‡	14.6 ± 2.0	20.4 ± 1.9*
Effective stroke volume, *ml*	13.1 ± 1.1	9.2 ± 1.3*	14.6 ± 2.0	10.5 ± 1.5*
Regurgitant stroke volume, *ml*	—	12.3 ± 0.7	—	10.0 ± 0.5
Effective cardiac index, *liter/min per m²*	2.11 ± 0.17	1.50 ± 0.22*	2.70 ± 0.37	1.90 ± 0.25*
Ejection fraction, stroke volume/end-diastolic volume	0.40 ± 0.05	0.65 ± 0.06‡	0.45 ± 0.05	0.61 ± 0.01‡
Total peak flow, *ml/sec*	113 ± 8	156 ± 12‡	143 ± 15	195 ± 14*
Aortic peak flow, *ml/sec*	113 ± 8	156 ± 12‡	143 ± 15	143 ± 13
Peak LV wall tension, *g/cm²*	170 ± 22	146 ± 19‡	152 ± 11	124 ± 11‡
Integrated LV wall tension, *g sec/cm²*	30.4 ± 4.3	24.0 ± 3.3‡	24.7 ± 2.3	16.1 ± 1.5‡
Peak circumferential fiber-shortening velocity, *cm/sec*	9.95 ± 0.96	15.05 ± 1.44‡	13.12 ± 1.50	17.89 ± 0.81*
Peak contractile element velocity during ejection, *cm/sec*	9.39 ± 0.73	14.36 ± 1.11‡	12.94 ± 1.88	16.63 ± 1.47‡
Peak contractile element power, *g cm/sec*	1604 ± 238	1923 ± 197‡	1970 ± 213	2018 ± 185
Contractile element work, *g cm*	230 ± 31	264 ± 31‡	229 ± 26	194 ± 21
Circumferential fiber work, *g cm*	172 ± 26	227 ± 25‡	185 ± 23	186 ± 22
Circumferential fiber work/ contractile element work	0.74 ± 0.04	0.87 ± 0.03‡	0.81 ± 0.02	0.95 ± 0.02‡
$\int T / \int LVP$, *g/cm² per g per cm²*	1.36 ± 0.09	1.20 ± 0.11‡	1.44 ± 0.08	1.36 ± 0.07
V_{max}, *cm/sec*	41 ± 2	41 ± 2	42 ± 2	43 ± 1

Comparing AI (nine experiments) or MI (six experiments) with control.

* $P < 0.05$.

‡ $P < 0.01$.

6B). Since MI augmented the extent of LV emptying (Fig. 6C), LV peak and integrated tensions were reduced relatively more than LV pressure (Fig. 5E). Furthermore, the combination of a decrease in LV pressure during ejection and the marked reduction in LV volume resulted in a precipitous decline in LV tension during the course of ejection. As with AI, the ratio of integrated wall tension to integrated LV pressure declined, but to a lesser degree, from an average of 1.44 during the control period to 1.36 in MI, and the ejection fraction increased from 0.45 to 0.61. As with AI, MI increased V_{CF} (Figs. 6D and 6F) and the extent of fiber shortening. Contractility was evaluated by the extrapolation to zero tension of the force-velocity relation from the isovolumic portions of the beats. V_{max} thus calculated was unchanged, averaging 42 ± 2 cm/sec in the control period and 43 ± 1 cm/sec with MI.

DISCUSSION

From the present study it is evident that the acute production of hemodynamic abnormalities resembling aortic or mitral valvular regurgitation results in complex alterations in the mechanical behavior of the left ventricle. Although significant hemodynamic alterations occur, it appears that neither acutely induced AI or MI alter the contractile state of the myocardium, as reflected in the force-velocity relation and the maximum velocity of shortening of the unloaded contractile elements of the myocardium (V_{max}) (19). Thus, neither AI nor MI altered calculated V_{max}. Furthermore, in both states the LV fibers shortened to the same isovolumic length-tension line as was observed in the control period rather than beyond it, as would have occurred with an increase in contractility; these observations were made both in the presence and absence of beta adrenergic blockade, and were

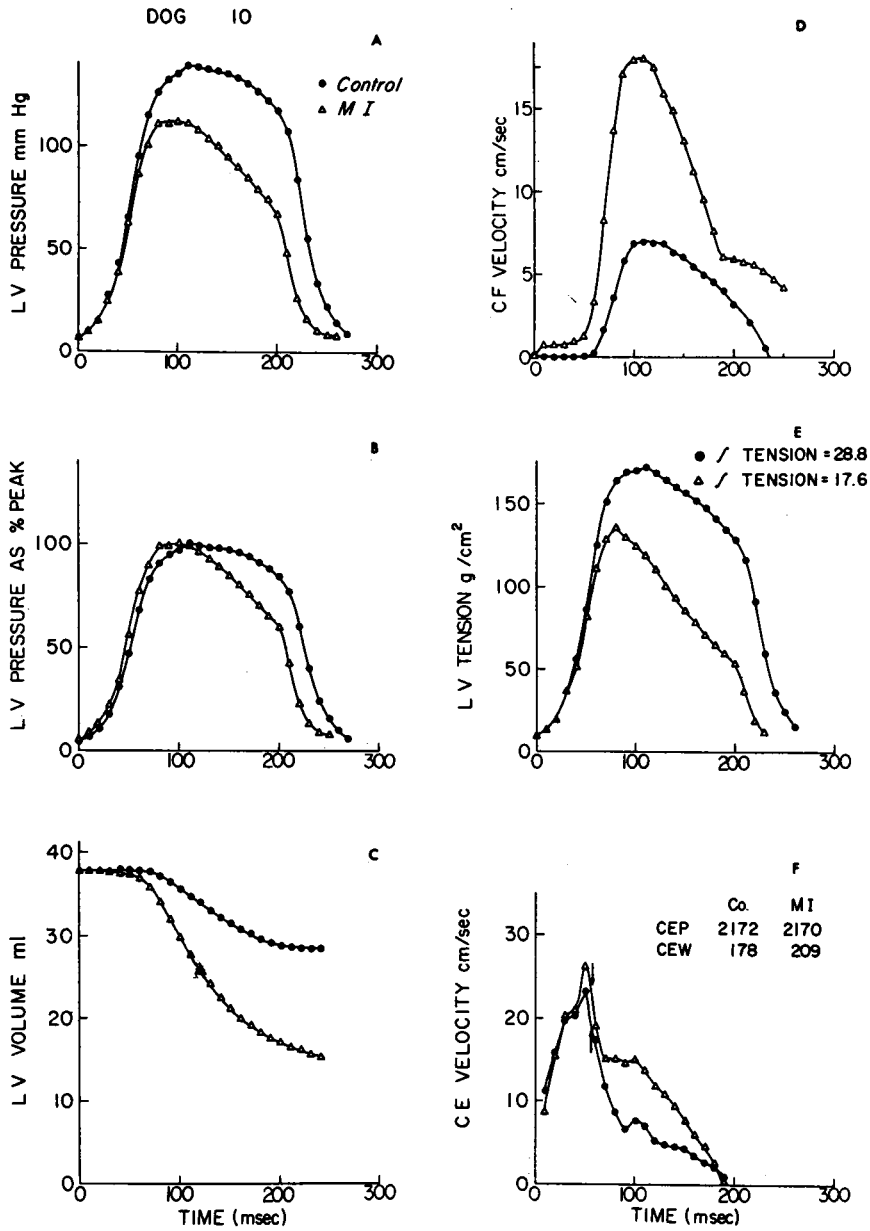

FIGURE 6 Comparison of a control beat and MI at the same end-diastolic volume.

therefore not dependent on reflex changes in myocardial contractility. In the presence of decreased cardiac output with AI and MI the possibility that a decrease in coronary blood flow might have occurred was considered, but was thought to be very unlikely in view of other studies which have demonstrated that coronary flow actually increases under these circumstances (31, 32).

In the absence of alterations in the contractile state of the myocardium the profound alterations in the behavior of the ventricles are best attributed to the marked changes in the instantaneous load placed on the myocardium (16) by the production of the regurgitant lesions. Both valvular lesions reduce the impedance to LV emptying, AI by reducing the pressure and volume in the aorta at the onset of ventricular ejection, and MI by providing a low-resistance outflow path in parallel with the systemic circuit.

The alteration in the load occurs by two separate

mechanisms. The first, present with "free" AI and "free" MI consists of an increase in preload, and therefore, ventricular volume. Ventricular volume remained greater in the presence of both AI and MI throughout all but the very last portion of systole (Fig. 3D). With the higher volumes, ventricular radii, and unchanged left ventricular peak pressures, peak wall tension was elevated above control levels with both lesions. However, the ratio of integrated tension to integrated pressure fell with the induction of both AI and MI, indicating that despite elevated peak tensions, average tension was decreased in relation to average pressure.

In order to clarify the effects of afterload independently of altered preload, AI or MI were compared with the control state at equivalent end-diastolic volumes. Under these conditions, both AI and MI resulted in an augmentation of total ventricular stroke volume, that is, in the magnitude of the systolic reduction of ventricular volume, despite the fact that the contractile state of the myocardium was unaltered. The effect is best illustrated by Fig. 5 where LV pressure was identical in the control state and in the presence of AI. However, due to the more rapid decrease in ventricular volume in AI and MI, a striking reduction in wall tension occurred. This more rapid decline in wall tension despite unchanged intraventricular pressure serves to explain the fall in the ratio of integrated tension/pressure. Therefore, because of the rapid ejection, tension either falls more rapidly at equivalent preloads or rises less than would be expected from the increased ventricular size of free AI or MI (33).

Concomitant with the changes in wall tension, circumferential fiber velocity increased in AI and MI. With "free" AI or MI, part of this increase can be attributed, on the basis of studies on isolated cardiac muscle (19), to the longer instantaneous fiber length. Conversely, with AI and MI compared with control at equivalent preload, the higher V_{CF} would appear to be due to the lower instantaneous wall tensions. This effect of the lower wall tension also has its counterpart in isolated muscle, in which contractile activity can be expressed either in the development of tension or shortening (34), and both the extent and velocity of myocardial fiber shortening are inversely related to tension developed (18). The reduction in instantaneous wall tension consequent to a sudden reduction in aortic pressure (16) or to valvular regurgitation in the steady state thus permits the contractile activity to be manifest by a greater extent and velocity of fiber shortening. This creates what could be considered to be a positive feedback mechanism, in that the enhanced fiber shortening further reduces tension, which in turn further enhances shortening until the contractile activity ceases at the cessation of the active state.

It should be noted that in the intact heart tension and circumferential fiber-shortening velocity are interdependent variables, whereas in isolated papillary muscle preparations the velocity of shortening during isotonic contraction is a dependent function of tension alone at equal muscle lengths. In the intact heart the ventricle generates its own load in part, since during ejection, ventricular systolic pressure is proportional to the product of instantaneous flow and the impedance. Thus, a rapid ejection into the aorta will result in higher aortic and left ventricular pressures than a slower ejection. On the other hand, with a low impedance to ejection, as occurs with AI or MI, a higher ejection velocity is required to achieve the same intraventricular pressure.

The possibility, therefore, exists that the velocity of shortening at a given length is no longer a simple function of tension. This is illustrated in Fig. 5. In both the control and AI beats, ventricular ejection had commenced by 90 msec (panel D). Tension is nearly identical (panel E), whereas myocardial fiber length is slightly shorter in the AI beat (panel C). Despite shorter fiber length in AI and almost identical tensions (panel E), the velocity of contractile element shortening is considerably greater during AI. A similar observation is shown in Fig. 7 where the length-tension curves from two control and two AI beats are plotted. For these beats the course of fiber shortening along the length-tension curves consistently followed a common pathway. V_{CF} and V_{CE} averaged 34% higher in the AI beats at lengths and tensions equal to those occurring in the control period.

This interdependence of force and velocity with length and impedance is of interest in conjunction with the striking acceleration in V_{CE} that accompanies ejection in the intact heart, despite constant or rising tension (Figs. 4C, 5F, and 6F).

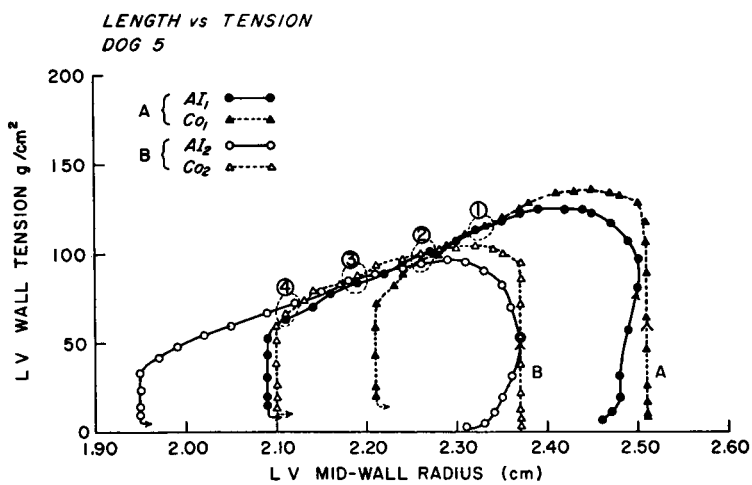

FIGURE 7 Length-tension relations during ejection in control beats and AI: two pairs of control (triangles) and AI beats (circles), each pair from the same end-diastolic volume (A = 31 ml, B = 23 ml) are plotted as length (mid-wall radius) vs. tension. Despite the similarities between length and LV wall tension, the circumferential fiber and contractile element velocities for the AI beats were, on the average, 34% higher at the four equivalent length-tension points indicated by the numbers in the figure. For example, at point 2, at an instantaneous LV mid-wall radius of 2.28 cm, V_{CE} in the control beats from an end-diastolic radius of 2.37 (open triangles) equalled 6.8 and 10.2 cm/sec in that from an end-diastolic radius of 2.51 cm (closed triangles). In contrast, with AI, V_{CE} was 11.2 and 13.0 cm/sec, respectively, from similar end-diastolic fiber lengths.

An earlier study on the effects of afterload on the mechanics of ventricular ejection (16) first called attention to this apparent deviation of velocity of shortening from the isovolumic inverse force–velocity relation during ejection. This deviation of velocity of shortening is roughly inversely proportional to the impedance and finds its parallel in the isolated papillary muscle preparation (16, 35). It is, therefore, evident that the velocity of shortening can be shown to be a rough inverse function of tension at a given length (Fig. 8). This general relation must also be expanded to include the possibility that the velocity of shortening and, therefore, the magnitude of shortening and contractile element work is a function of both tension and impedance.

In addition to alteration of myocardial performance secondary to the effects of altered impedance on V_{CE}, the internal transfer of energy between the contractile elements and the fiber may also be altered in the presence of valvular regurgitation. In A. V. Hill's model for muscle (28), the series elastic component is stretched during isovolumic contraction, absorbing contractile element work, while during late ejection a fraction of this work is regained (Fig. 9A). The ratio of fiber-shortening work to contractile element work is a measure of the efficiency of this energy transfer through the

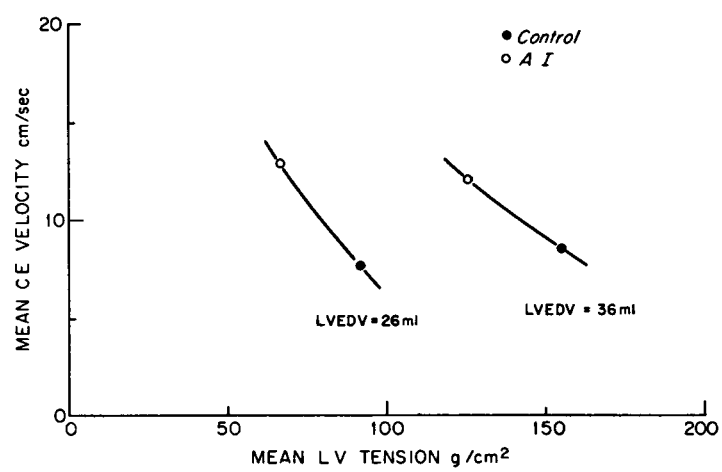

FIGURE 8 Mean force-velocity relations in control beats and AI: average contractile element (CE) velocity during ejection is plotted as a function of average wall tension for control (closed circles) and AI (open circles) at two end-diastolic volumes (LVEDV) in three dogs. The manner in which V_{CE} is dependent on load despite unchanged end-diastolic volume and contractility parallels the inverse force–velocity relation of isolated papillary muscle.

series elastic component. As noted in Fig. 9B, the efficiency of this transfer was increased significantly, from 0.79, in six experiments during the control period, to 0.86 in AI and to 0.99 in MI. This increased efficiency in the transfer of mechanical energy across the series elastic results in part from the relatively lower tension in the presence of AI and MI, with, therefore, less stretching of the SE. Further, since shortening continued to a lower tension, a greater percentage of the energy stored in the SE was regained as external work. Due to this improved energy transfer a given amount of CE work resulted in a greater amount of fiber-shortening work. This illustrates the interesting paradox that whereas the effectiveness of the ventricle as a pump may be reduced by valvular regurgitation, the efficiency of internal energy transfer is actually increased.

Several qualifications are pertinent before applying these findings to clinical AI or MI, in as much as the effects of heart rate, anesthesia, myocardial hypertrophy, and the duration of the lesion are still to be evaluated. However, recent studies have illustrated the qualitative and quantitative similarity of induced changes in the force-velocity relation in conscious animals (23) and man (36) to those in anesthetized open-chest animals. Application of the results to clinical states must, therefore, be evaluated in the light of potential compensatory mechanisms which may themselves be revealed by deviations from the controlled experiment. Of prime interest in this regard is the observation that both AI and MI resulted in an increased ejection fraction. This ratio has been used as an index of contractility in patients with a variety of disease states, including valvular regurgitation (7, 9). In the present study, an increase in ejection fraction occurred, despite the fact that the basic contractile state of the ventricle was unaltered, and took place as a consequence of the aforementioned reductions in impedance to ejection. Thus, at least under the conditions of these experiments, and theoretically in the presence of chronic regurgitation as well, a normal ejection fraction might indicate an impaired, rather than a normal contractile state. However, the relative rarity of supranormal ejection fractions in patients studied with AI and MI suggests the possibility that changes in contractility occurring in chronic regurgitation have obscured the primary

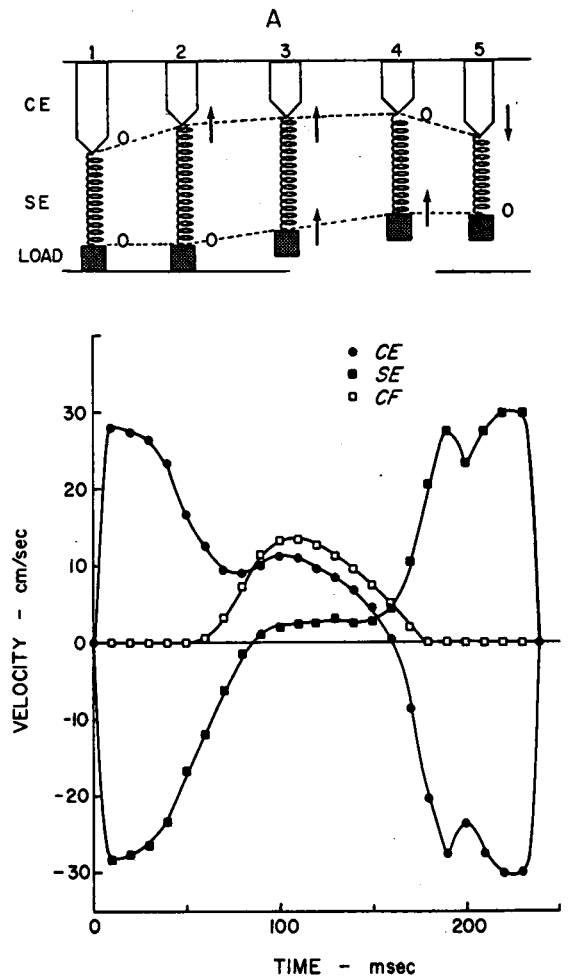

FIGURE 9A Contractile element (CE), series elastic (SE), and fiber-shortening interrelations: panel A, illustrates diagrammatically and with data from a typical beat, the application of the Hill model to the intact heart. In this model seen at rest in 1 (top), the muscle is considered to consist of a CE which is connected to the load by a spring-like series SE. During isovolumic contraction, 2, the CE shortens (closed circles, bottom) the energy of which is stored in the SE (closed squares) which has been stretched. During shortening, 3, some of the energy generated by the CE continues to stretch the spring (SE) up to the point of peak tension (indicated by an arrow in the bottom portion of the figure) at which points some of the energy stored in the SE is regained, causing fiber-shortening velocity to exceed CE velocity. By the end of ejection, 4, the CE is no longer shortening and the latter portion of fiber shortening is due to the recoiling SE. During isovolumic relaxation, 5, the SE continues to recoil maintaining tension and stretching the CE.

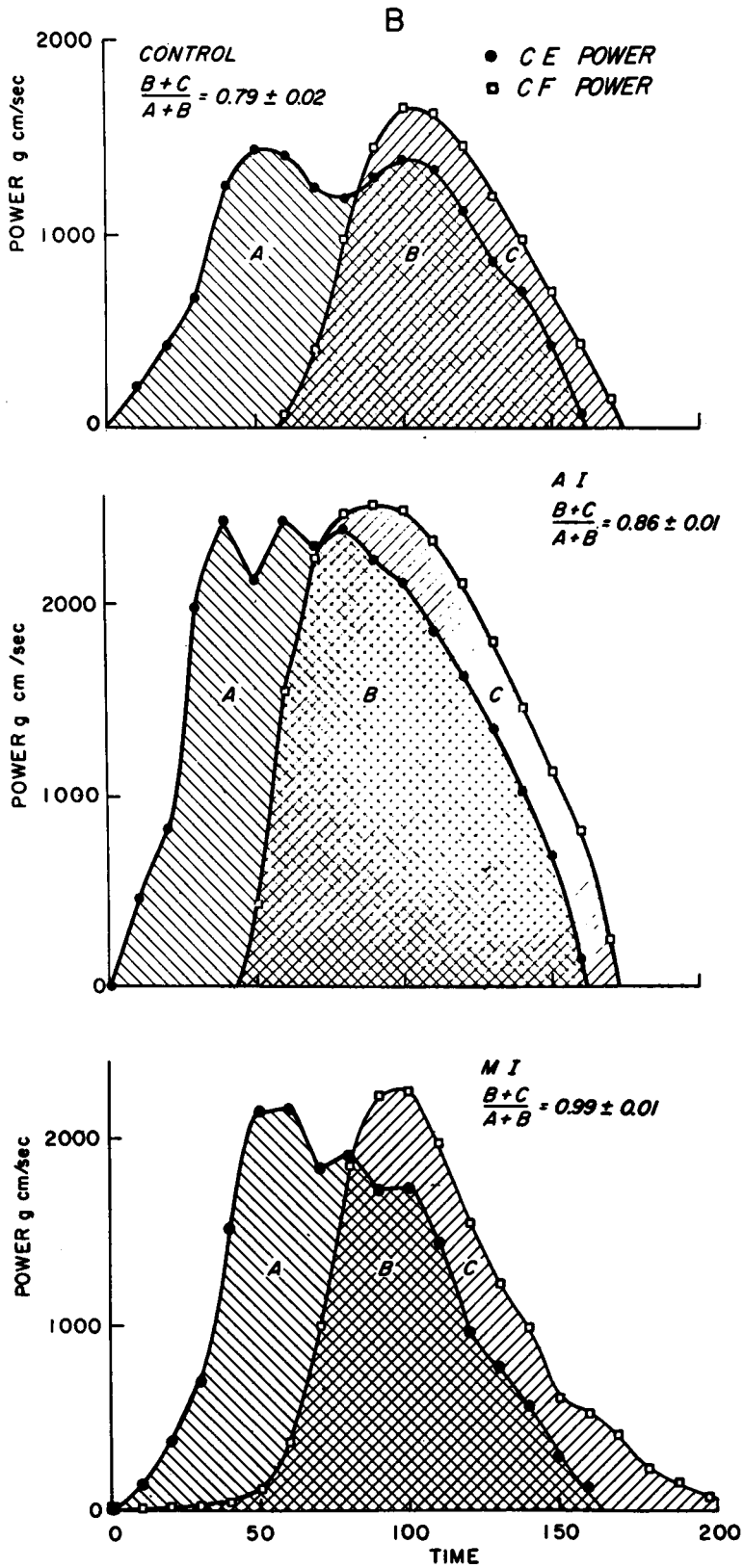

FIGURE 9B The degree to which CE energy is translated into fiber shortening is seen as the ratio of fiber-shortening work to CE work. Panel B illustrates calculated CE and fiber shortening from a control beat (top), AI (middle), and MI (bottom). A = CE work performed upon SE. B = CE work directly resulting in fiber shortening. C = fiber shortening work resulting from recoil of the SE. B + C = total fiber shortening work. A + B = total contractile element work.

mechanical changes secondary to the altered loading. Further, it is clear that measures of external performance, such as stroke work and ejection fraction, are as dependent upon instantaneous impedance as upon myocardial contractility. Accordingly, in the presence of valvular heart disease, in which profound changes in impedance occur, traditional measures of contractility may not provide an accurate description of muscle performance. It appears likely that applications to man of the concepts of myocardial mechanics as employed in the present study are possible, by means of cineangiographic techniques that allow measurement of fiber length, shortening velocity, and tension (36), and may provide further insight into chronic derangements of ventricular contraction.

ACKNOWLEDGMENTS

The technical assistance of Robert M. Lewis and Richard D. McGill is gratefully acknowledged. The assistance of Miss Virginia Aandahl with computer programming is appreciated.

REFERENCES

1. Braunwald, E., and A. G. Morrow. 1958. A method for the detection and estimation of aortic regurgitant flow in man. *Circulation.* **17:** 505.
2. Warner, H. R., and A. F. Toronto. 1961. Effect of heart rate on aortic insufficiency as measured by a dye dilution technique. *Circulation Res.* **9:** 413.
3. Sandler, H., H. T. Dodge, R. E. Hay, and C. E. Rackley. 1963. Quantitation of valvular insufficiency in man by angiocardiography *Am. Heart J.* **65:** 501.
4. Braunwald, E., G. H. Welch, Jr., and S. J. Sarnoff. 1957. Hemodynamic effects of quantitatively varied experimental mitral regurgitation. *Circulation Res.* **5:** 539.
5. Welch, G. H., Jr., E. Braunwald, and S. J. Sarnoff. 1957. Hemodynamic effects of quantitatively varied experimental aortic regurgitation. *Circulation Res.* **5:** 546.
6. Ross, J., Jr., T. Cooper, and C. R. Lombardo. 1960. Hemodynamic observations in experimental mitral regurgitation. *Surgery.* **47:** 795.
7. Jones, J. W., C. E. Rackley, R. A. Bruce, H. T. Dodge, L. A. Cobb, and H. Sandler. 1964. Left ventricular volumes in valvular heart disease. *Circulation.* **29:** 887.
8. Miller, G. A. H., R. Brown, and H. J. C. Swan. 1964. Isolated congenital mitral insufficiency with particular reference to left heart volumes. *Circulation.* **29:** 356.
9. Miller, G. A. H., J. W. Kirklin, and H. J. C. Swan. 1965. Myocardial function and left ventricular volumes in acquired valvular insufficiency. *Circulation.* **31:** 374.
10. Imperial, E. S., M. N. Levy, and H. Zieske, Jr. 1961. Outflow resistance as an independent determinant of cardiac performance. *Circulation Res.* **9:** 1148.
11. Sonnenblick, E. H., and S. E. Downing. 1963. Afterload as a primary determinant of ventricular performance. *Am. J. Physiol.* **204:** 604.
12. Wilcken, D. E. L., A. A. Charlier, J. I. E. Hoffman, and A. Guz. 1964. Effects of alterations in aortic impedance on the performance of the ventricles. *Circulation Res.* **14:** 283.
13. Wilcken, D. E. L. 1965. Load, work, and velocity of muscle shortening of the left ventricle in normal and abnormal human hearts. *J. Clin. Invest.* **44:** 1295.
14. Fry, D. L., D. M. Griggs, Jr., and J. C. Greenfield. 1964. Myocardial mechanics: tension-velocity-length relationships of heart muscle. *Circulation Res.* **14:** 73.
15. Levine, H. J., and N. A. Britman. Force-velocity relations in the intact dog heart. *J. Clin. Invest.* **43:** 1383.
16. Ross, J., Jr., J. W. Covell, E. H. Sonnenblick, and E. Braunwald. 1966. Contractile state of the heart characterized by force-velocity relations in variably afterloaded and isovolumic beats. *Circulation Res.* **18:** 149.
17. Covell, J. W., J. Ross, Jr., E. H. Sonnenblick, and E. Braunwald. 1966. Comparison of the force-velocity relation and the ventricular function curve as measures of the contractile state of the intact heart *Circulation Res.* **19:** 364.
18. Sonnenblick, E. H. 1962. Implications of muscle mechanics in the heart. *Federation Proc.* **21:** 975.
19. Sonnenblick, E. H. 1965. Determinants of active state in heart muscle: force velocity, instantaneous muscle length, time. *Federation Proc.* **24:** 1396.
20. Monroe, R. G., and G. N. French. 1961. Left ventricular pressure-volume relationships and myocardial oxygen consumption in the isolated heart. *Circulation Res.* **9:** 362.
21. Taylor, R. R., and J. Ross, Jr. 1967. A comparison of the left ventricular isovolumic and auxotonic volume-tension diagrams in the intact dog. *Physiologist.* **10:** 322. (Abstr.)
22. Sandler, H., and H. T. Dodge. 1963. Left ventricular tension and stress in man. *Circulation Res.* **13:** 91.
23. Taylor, R. R., J. Ross, Jr., J. W. Covell, and E. H. Sonnenblick. 1967. A quantitative analysis of left ventricular myocardial function in the intact, sedated dog. *Circulation Res.* **21:** 99.
24. Rushmer, R. F. 1956. Initial phase of ventricular systole: asynchronous contraction. *Am. J. Physiol.* **184:** 188.
25. Ninomiya, I., and M. F. Wilson. 1965. Analysis of ventricular dimension in the unanesthetized dog. *Circulation Res.* **16:** 249.
26. Hawthorne, E. W. 1966. Symposium on measurements of left ventricular volume. III. Dynamic geometry of the left ventricle. *Am. J. Cardiol.* **18:** 566.
27. Gorlin, R., E. L. Rolett, P. M. Yurchak, and W. Elliott. 1964. Left ventricular volume in man measured by thermodilution. *J. Clin. Invest.* **43:** 1203.
28. Hill, A. V. 1938. The heat of shortening and the dynamic constants of muscle. *Proc. Roy. Soc. (London). Ser. B.* **126:** 136.
29. Covell, J. W., R. R. Taylor, and J. Ross, Jr. 1967. Series elasticity in the intact left ventricle determined

by a quick release technique. *Federation Proc.* **26**: 382. (Abstr.)
30. Sonnenblick, E. H. 1964. Series elastic and contractile elements in heart muscle: changes in muscle length. *Am. J. Physiol.* **207**: 1330.
31. Wégria, R., G. Muelheims, R. Jreissaty, and J. Nakano. 1958. Effect of acute mitral insufficiency of various degrees on mean arterial blood pressure, coronary blood flow, cardiac output and oxygen consumption. *Circulation Res.* **6**: 301.
32. Wegria, R., G. Muelheims, J. R. Golub, R. Jreissaty, and J. Nakano. 1958. Effect of aortic insufficiency on arterial blood pressure, coronary blood flow and cardiac oxygen consumption. *J. Clin. Invest.* **37**: 471.
33. Markovskaya, G. I., V. V. Solov'ev, S. M. Shenderov, A. A. Gorbachenkov, Yu. S. Mdinaradze, F. I. Zargarli, A. L. Mikoelyan, and E. B. Shul'zhenko. 1966. Cardiac hyperfunction and insufficiency in experimental valvular lesions. *Kardiologiya.* 1965, **5**: 8. Translated in: *Federation Proc.* (Translation Supplement) **25**: T615.
34. Downing, S. E., and E. H. Sonnenblick. 1964. Cardiac muscle mechanics and ventricular performance: force and time parameters. *Am. J. Physiol.* **207**: 705.
35. Parmley, W. W., and E. H. Sonnenblick. 1967. Series elasticity in heart muscle: its relation to contractile element velocity and proposed muscle models. *Circulation Res.* **20**: 112.
36. Gault, J. H., J. Ross, Jr., E. H. Sonnenblick, and E. Braunwald. 1966. Characterization of myocardial contractility in patients with and without cardiac dysfunction by the instantaneous tension-velocity relation. *Circulation.* **34** (Suppl. 3): III-108. (Abstr.)